American Mineralogist, Volume 71, pages 1210–1213, 1986

Visualizing low symmetry of a grandite garnet on precession photographs

HISAKO HIRAI
Institute of Geoscience, University of Tsukuba, Ibaraki 305, Japan
HIROMOTO NAKAZAWA
National Institute for Research in Inorganic Materials, Namiki 1-1, Sakura-mura, Niihari-gun, Ibaraki 305, Japan

ABSTRACT

Low symmetry of a grandite garnet, $An_{50}Gr_{45}Sp_5$, from Mul-Kum mine, South Korea, showing an "optical anomaly," was observed by conventional precession methods. A series of forbidden reflections in cubic symmetry (*Ia3d*) was clearly observed on the photographs. The symmetry determined by taking into account these extra reflections is orthorhombic (*Fddd*). The grandite garnet has an exsolution texture consisting of thin lamellae and host. The forbidden reflections are ascribed to both the lamellae and host. Appreciating the slight difference in intensity among the reflections equivalent in *Fddd,* the symmetries of both or one phase may even be lower than orthorhombic, probably *C2/c.* The present observations of the grandite garnet have straightforwardly established the existence of its noncubic structure.

INTRODUCTION

Symmetry of garnet has long been known to be cubic with space group of *Ia3d,* since Menzer (1926) determined its crystal structure. Some lower-symmetry structures are, however, known for the high-pressure phases of $CdGeO_3$ and $CaGeO_3$ ($I4_1/a$) (Prewitt and Sleight, 1969) and for henritermierite, $Ca_3(Mn_{1.5}Al_{0.5})(SiO_4)_2(OH)_4$ ($I4_1/acd$) (Aubry et al., 1969), which are derivatives of the garnet structure. Pyrope-grossular garnet ($Py_{90}Gr_{10}$) is cubic ($I2_13$) but has lower symmetry than *Ia3d* (Dempsey, 1980). In the grandite garnet series (andradite-grossular, $Ca_3Fe_2Si_3O_{12}$-$Ca_3Al_2Si_3O_{12}$), birefringence is commonly observed under the optical microscope and has been generally regarded as an optical anomaly, possibly due to strain. However, the optical anomaly was recently explained to be due to lowering the symmetry of the grandite garnet to orthorhombic (*Fddd*) or triclinic ($I\bar{1}$) associated with ordering of Fe and Al (Miyazaki et al., 1975; Takéuchi and Haga, 1976; Takéuchi et al., 1982). The lower symmetry was, however, not obvious since extra reflections forbidden to *Ia3d* symmetry were not present; the lower symmetry was only recognized by a slight difference in X-ray diffraction intensities of equivalent reflections in *Ia3d* using four-circle diffractometry. In the present study a series of forbidden reflections in the cubic space group *Ia3d* was clearly observed in X-ray precession photographs of a grandite garnet, giving direct visual evidence for noncubic symmetry of the garnet.

EXPERIMENTAL PROCEDURES

Polarizing microscopic observation and chemical analysis

The grandite garnet studied was collected by H. Honma at the Mul-Kum mine, South Korea. Thin sections, parallel to (110), (111), and (100), were prepared from a large dodecahedral crystal (~6 mm in diameter). Miller indices used in this paper refer to the pseudocubic symmetry. Compositional zoning is well defined, and the mean chemical composition of the zones measured by electron-probe microanalysis (EPMA) is $An_{50}Gr_{45}Sp_5$. Under crossed polars, the tweed-like texture consists of two differently oriented lamellae and host (Fig. 1a). The thickness of the lamellae is a few micronmeters (more than 5 μm is rare). Both lamellae and host show birefringence. The back-scattered electron image (BEI) of the area shown in Figure 1a was obtained by SEM (Fig. 1b). To confirm the compositional difference, the intensity distribution of characteristic X-rays of Fe and Al was examined along the line drawn in Fig. 1b. An inverse relationship between Fe and Al was obviously found across the lamellae (Fig. 1c). Quantitative analyses were carried out by EPMA at each lamella and

Table 1. Selected chemical compositions of the tweed-like texture measured by EPMA

	Lamellae			Host		
	l_1	l_3	l_4	m_1	m_4	m_5
SiO_2	36.08	35.86	36.83	36.99	37.00	36.61
TiO_2	n.d.	n.d.	n.d.	n.d.	n.d.	n.d.
Al_2O_3	8.77	8.90	9.02	10.19	10.27	10.23
Fe_2O_3	19.72	19.50	19.68	17.57	17.56	17.29
Cr_2O_3	n.d.	n.d.	n.d.	n.d.	n.d.	n.d.
MnO	2.31	2.13	2.12	2.51	2.61	2.60
MgO	n.d.	n.d.	n.d.	n.d.	n.d.	n.d.
CaO	31.83	31.94	32.29	31.95	32.13	31.56
Na_2O	n.d.	n.d.	n.d.	n.d.	n.d.	n.d.
K_2O	n.d.	n.d.	n.d.	n.d.	n.d.	n.d.
NiO	n.d.	n.d.	n.d.	n.d.	n.d.	n.d.
Total	98.81	98.34	99.94	99.22	99.56	98.39
An	58	58	58	52	52	51
Gr	37	37	37	42	42	43
Sp	5	5	5	6	6	6

Note: Analysis points (l_1, l_2, etc.) shown in Fig. 1c; n.d. = not detected.

0003–004X/86/0910–1210$02.00

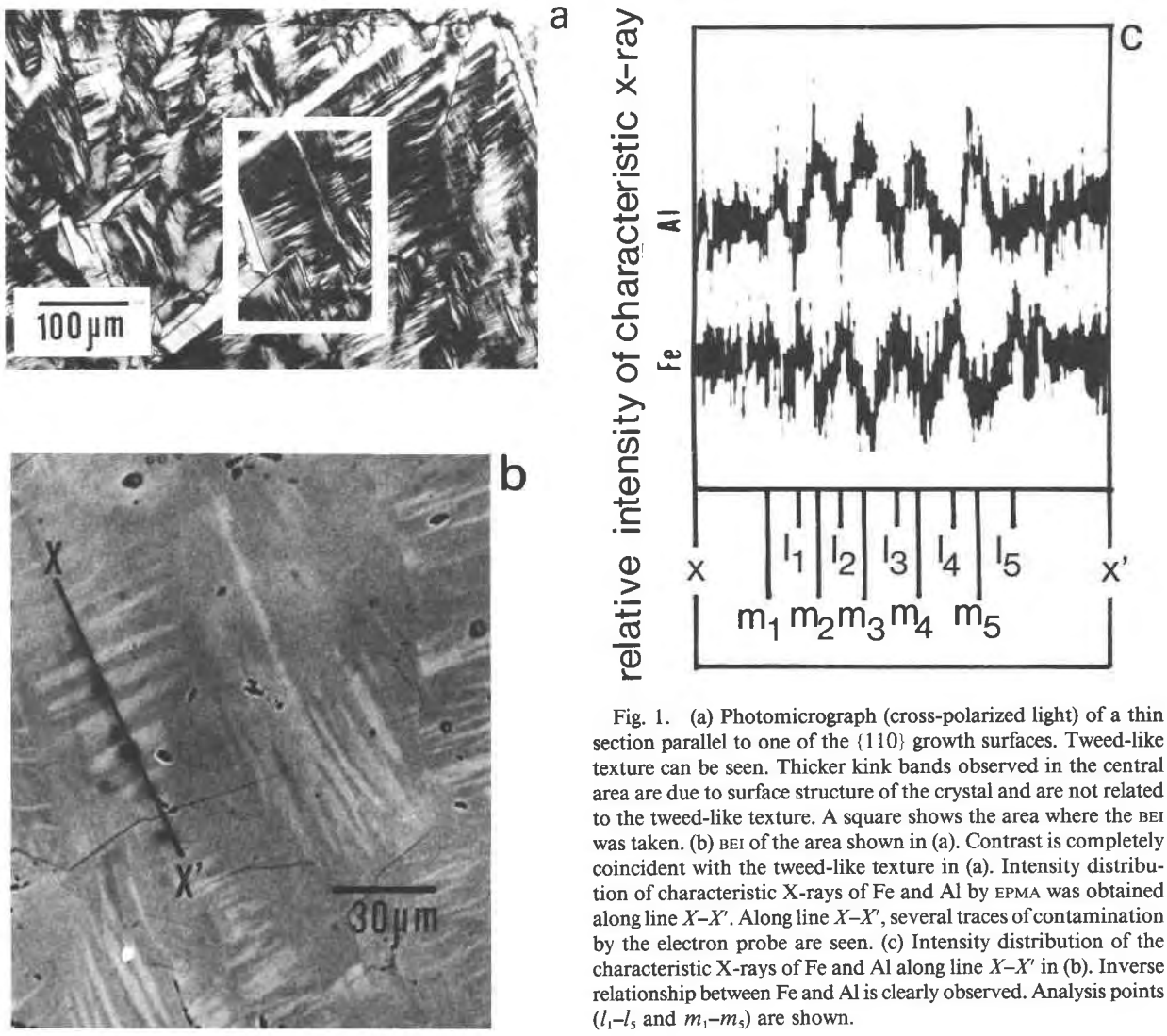

Fig. 1. (a) Photomicrograph (cross-polarized light) of a thin section parallel to one of the {110} growth surfaces. Tweed-like texture can be seen. Thicker kink bands observed in the central area are due to surface structure of the crystal and are not related to the tweed-like texture. A square shows the area where the BEI was taken. (b) BEI of the area shown in (a). Contrast is completely coincident with the tweed-like texture in (a). Intensity distribution of characteristic X-rays of Fe and Al by EPMA was obtained along line X–X'. Along line X–X', several traces of contamination by the electron probe are seen. (c) Intensity distribution of the characteristic X-rays of Fe and Al along line X–X' in (b). Inverse relationship between Fe and Al is clearly observed. Analysis points (l_1–l_5 and m_1–m_5) are shown.

host shown in Fig. 1c. The selected chemical compositions are given in Table 1. The mean chemical compositions for the lamellae and the host are $An_{58}Gr_{37}Sp_5$ and $An_{51}Gr_{43}Sp_6$, respectively. The chemical analyses revealed that the tweed-like texture consists of Fe-rich lamellae in an Fe-poor host.

In thin sections normal to the compositional zoning, the lamellae were found to extend across the boundaries of compositional zoning, indicating that the lamellae were formed not during but after the crystal growth (Fig. 2). These observations and chemical analyses suggest that the tweed-like texture is likely to be an exsolution texture. The presence of exsolution in grandite garnet has already been reported by Hirai et al. (1982) and Hirai and Nakazawa (1986).

X-ray diffraction study

After the polarizing microscopic observations and the chemical analyses, the specimen chips were removed from thin sections parallel to (110) and also parallel to (111). The specimens are rectangular plates with dimensions of about 120 × 100 × 30 μm. Precession photographs were taken using Zr-filtered Mo-$K\alpha$ radiation (45 kV, 150 mA, exposed for 50–70 h). The pseudocubic unit-cell parameter is 12.0 Å. Reflections forbidden to $Ia3d$ symmetry can be clearly observed in the photographs (Fig. 3). By several settings of crystal orientation, the forbidden reflections were confirmed not to result from double reflections. All reflections, forbidden and allowed, were accompanied by one or two tails, which is most easily observed in Figure 3a (see the arrows labeled 1 and 2). The spot (head) and tail may correspond to the reflections from the host and the lamellae, respectively, considering the volume ratio of the host to the lamellae and the intensity ratio of the spot to the tail. The difference in cell dimension between the spot and the tail is estimated to be about 0.02 Å by comparing the intervals between the spots and the tails in Friedel-pair reflections. The tail has the larger cell dimension. The difference estimated in cell dimension agrees with that estimated from the compositional difference measured by EPMA in the tweed-like texture.

The extra reflections are all of the type $h + k + l = 2n$, but they violate the extinction rules of $Ia3d$: for $0kl$, $k,l = 2n$ and for hhl, $2h + l = 4n$. Presence or absence of forbidden reflections

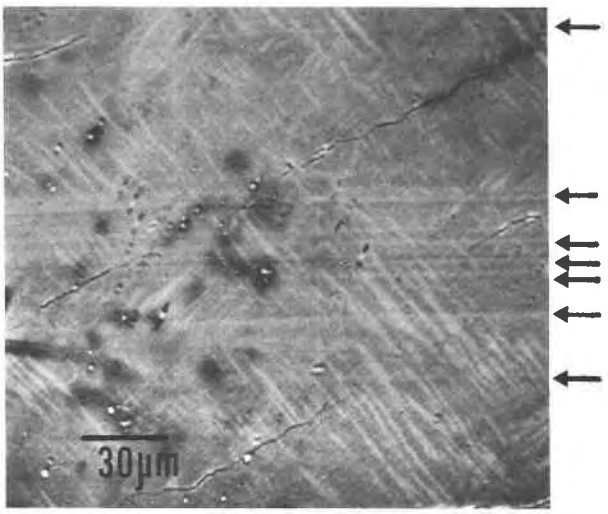

Fig. 2. BEI of the thin section normal to the compositional zoning. The arrows indicate the boundaries of the compositional zoning. Note that the lamellae extend throughout the several zones.

Table 2. List of extinction rules observed

*Ia*3*d*		Observed	
hkl:	$h + k + l = 2n$	*hkl*:	$h + k + l = 2n$
0*kl*:	$k, l = 2n$	0*kl*:	$k, l = 2n$
		*h*0*l*:	$h, l \neq 2n$
		*hk*0:	$h, k \neq 2n$
hhl:	$2h + l = 4n$	*hhl*:	$2h + l \neq 4n$
		$h\bar{h}l$:	$2h + l \neq 4n$
		lkl:	$2l + k \neq 4n$
		$lk\bar{l}$:	$2l + k \neq 4n$
		hkk:	$2k + h = 4n$
		$hk\bar{k}$:	$2k + h = 4n$

is summarized in Table 2, compared to those of *Ia*3*d*. The existence of the extra reflections means loss of several symmetry elements in *Ia*3*d*: all threefold symmetry axes, two of three *a*-glide planes and four of six *d*-glide planes (Fig. 3, Table 2). Diffraction symmetry is thus *mmm*, and the space group derived from the extinction rule is *Fddd*. The relationship of crystal axes between the orthorhombic and pseudocubic cells is $\mathbf{a}_{orth} = \mathbf{b}_{cub} + \mathbf{c}_{cub}$, $\mathbf{b}_{orth} = \mathbf{a}_{cub}$, and $\mathbf{c}_{orth} = \mathbf{c}_{cub} - \mathbf{b}_{cub}$.

A slight difference in intensity could also be observed among several reflections equivalent in *Fddd*. This intensity difference is unlikely to be related to the absorption of X-rays due to the specimen shape. Assuming that the intensity difference is intrin-

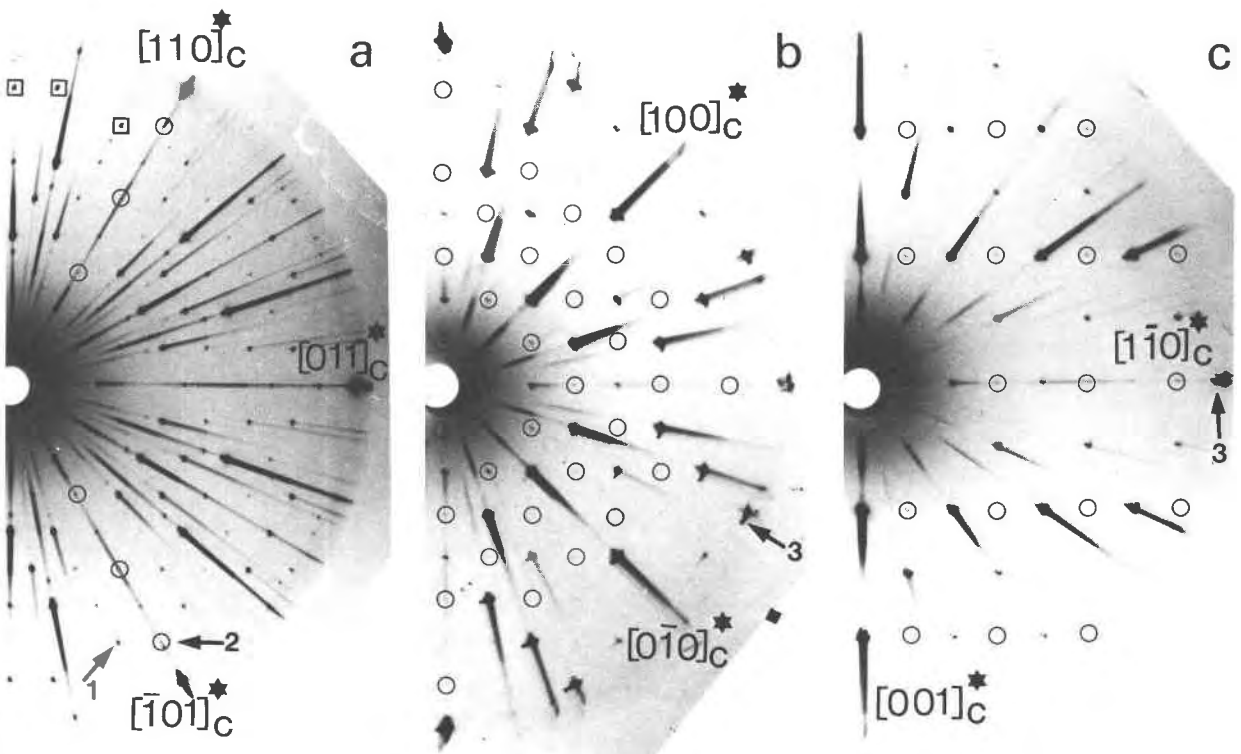

Fig. 3. The $hh\bar{h}$ (a), $hk0$ (b), and $h\bar{h}l$ (c) nets of the precession photographs. Miller indices used refer to the pseudocubic symmetry. The forbidden reflections are marked by circles. The arrows labeled 1 and 2 in (a) are the allowed and the forbidden reflections, respectively, in which the tail can easily be recognized. The arrows labeled 3 in (b) and (c) show splitting of spots along Debye-rings, probably due to misorientation among the compositional zones. (a) The forbidden reflections ($hk0$: $h, k \neq 2n$; $\bar{h}0\ l$: $h, l \neq 2n$) are observed, whereas the reflections of $0kl$: k, l are $2n$ only, giving a visual evidence for loss of a threefold symmetry axis. (b) The forbidden reflections ($hk0$: $h, k \neq 2n$) observed indicate loss of an *a*-glide plane. (c) The forbidden reflections ($h\bar{h}l$: $2h + l \neq 4n$) indicate loss of a *d*-glide plane.

sic, actual symmetry might be even lower than orthorhombic, probably monoclinic. In this case, the space group derived is $C2/c$, which is a subgroup of *Fddd*. The axial relation to the cubic cell is $\mathbf{a}_{mon} = \mathbf{a}_{cub}$, $\mathbf{b}_{mon} = \mathbf{b}_{cub} + \mathbf{c}_{cub}$, and $\mathbf{c}_{mon} = -\frac{1}{2}\mathbf{a}_{cub} + \frac{1}{2}\mathbf{b}_{cub} - \frac{1}{2}\mathbf{c}_{cub}$.

Discussion

The space group *Fddd* and its axial relations are the same as those described by previous workers (Miyazaki et al., 1975; Takéuchi and Haga, 1976; Takéuchi et al., 1982). The lower symmetry indicates an ordered arrangement of Fe and Al, as these octahedral sites are consequently differentiated into two nonequivalent sites. In the grandite garnet studied, the "forbidden reflections" are of sufficient intensity to be detected by conventional X-ray precession methods. A possible reason for this may be that the cation ordering of Fe and Al in this specimen is more complete than in other garnets, because deviation of the atomic coordinates from cubic is rather small (Takéuchi et al., 1982).

The garnet examined possesses the tweed-like texture interpreted as an exsolution texture mentioned above. The presence of the forbidden reflections in $Ia3d$ on the precession photographs provides distinct evidence for lower symmetry. This lower symmetry strongly supports an exsolution origin for the tweed-like texture. The specimen studied is not a single phase but includes two phases, the lamellae and the host. The tails, which can be regarded as reflections from the lamellae, were observed even in the forbidden (arrow labeled 2 in Fig. 3a) as well as in the allowed reflections (arrow labeled 1). It is therefore concluded that the symmetries of the host and lamellae are lowered at least to *Fddd*, but it is difficult at present to determine which probably has the even lower symmetry, $C2/c$. In any case, the present observations have straightforwardly established the existence of noncubic grandite garnet and its subsolidus decomposition.

Acknowledgments

The authors are grateful to Emeritus Professor Y. Takéuchi, University of Tokyo, for his valuable comments and critical reading of the manuscript and to Professor H. Honma, Tokyo Gakugei University, for his providing the hand specimens.

References

Aubry, André, Dusausoy, Yves, Laffaille, Alain, and Protas, Jean. (1969) Détermination et étude de la structure cristalline de l'henritermierite, hydrogrenat de symétrie quadratique. Bulletin de la Société française de Minéralogie et de Cristallographie, 92, 126–133.

Dempsey, M.J. (1980) Evidence for structural changes in garnet caused by calcium substitution. Contributions to Mineralogy and Petrology, 71, 281–282.

Hirai, Hisako, and Nakazawa, Hiromoto. (1986) Grandite garnet from Nevada: Confirmation of origin of iridescence by electron microscopy and interpretation of a moiré-like texture. American Mineralogist, 71, 123–26.

Hirai, Hisako, Sueno, Shigeho, and Nakazawa, Hiromoto. (1982) A lamellar texture with chemical contrast in grandite garnet from Nevada. American Mineralogist, 67, 1242–1247.

Menzer, G. (1926) Die Kristallstruktur von Granat. Zeitschrift für Kristallographie, 63, 157–158.

Miyazaki, Masaaki, Kihara, Kuniaki, Matsumoto, Takeo, and Sugiura, Seiji. (1975) X-ray diffraction symmetry of optically anomalous garnets. Crystallographic Society of Japan 1975 Annual Meeting (abstr. in Japanese), 19.

Prewitt, C.T., and Sleight, A.W. (1969) Garnet-like structures of high-pressure cadmium germanate and calcium germanate. Science, 163, 386–387.

Takéuchi, Yoshio, and Haga, Nobuhiko. (1976) Optical anomaly and structure of silicate garnets. Japan Academy Proceedings, 52, 228–231.

Takéuchi, Yoshio, Haga, Nobuhiko, Umizu, Shigetomo, and Sato, Gen. (1982) The derivative structure of silicate garnets in grandite. Zeitschrift für Kristallographie, 158, 53–99.

Manuscript received November 25, 1985
Manuscript accepted May 16, 1986